


Article

An Analytical Model for Stress and Curvature Prediction of a Strip Leveling Process

Shih-Kang Kuo¹, Yi-Liang Ou¹ and Dung-An Wang^{2,3,*} 

¹ Steel Research and Development Department, China Steel Corporation, Kaohsiung 81233, Taiwan; 150359@mail.csc.com.tw (S.-K.K.); 165688@mail.csc.com.tw (Y.-L.O.)

² Graduate Institute of Precision Engineering, National Chung Hsing University, 250 Kuo Kuang Rd., Taichung 40227, Taiwan

³ Faculty of Mechanical Engineering, Industrial University of Ho Chi Minh City, 12 Nguyen Van Bao, Ward 4, Go Vap District, Ho Chi Minh City 800010, Vietnam

* Correspondence: daw@dragon.nchu.edu.tw; Tel.: +886-4-22857207

Abstract: An analytical model of a steel strip under alternate bending/reverse bending during a roller leveling process is developed. A combined isotropic/kinematic hardening model is implemented through a combined hardening parameter. A formulation of the change of the effective stress as a function of the change of the effective strain under cyclic loading is combined with the developed analytical model to predict the stress distributions and residual curvature of a steel strip under roller leveling efficiently and accurately. Dissimilar to the commonly used assumption of one contact point between the stripe and the rolls, an effective radius modelling the wrap-around contact characteristics is proposed. An arc contact of the strip around a roll is described by the contact model. An oscillatory behavior of the residual curvature is observed when a range of roll intermesh setting is considered. The contact model added to the analytical model may enhance the accuracy in predicting the oscillatory behavior of the residual curvatures. A range of the roll intermesh setting can be suggested by the developed model to obtain a flat strip after roller leveling.

Keywords: roller leveling; steel strip; combined hardening; analytical model



Citation: Kuo, S.-K.; Ou, Y.-L.; Wang, D.-A. An Analytical Model for Stress and Curvature Prediction of a Strip Leveling Process. *Metals* **2022**, *12*, 757. <https://doi.org/10.3390/met12050757>

Academic Editors: George A. Pantazopoulos and Zhengyi Jiang

Received: 14 March 2022

Accepted: 24 April 2022

Published: 28 April 2022

Publisher's Note: MDPI stays neutral with regard to jurisdictional claims in published maps and institutional affiliations.



Copyright: © 2022 by the authors. Licensee MDPI, Basel, Switzerland. This article is an open access article distributed under the terms and conditions of the Creative Commons Attribution (CC BY) license (<https://creativecommons.org/licenses/by/4.0/>).

1. Introduction

Steel strips after rolling and annealing may possess defects such as wavy edges, center buckles, cambers, and twists. The flatness defects can be corrected by leveling in steel mills. Amor et al. [1] reported that shape defects of metal strips after rolling process or coiling operation can be removed by leveling in order to meet the quality requirement. Customers may cut the as-received flat stripes in order to achieve end functionalities. Unacceptable shape defects found after cutting the strips are serious issues of concern raised by the customers of steel mills. Li et al. [2] reported that these flatness/shape defects are mainly due to residual stresses generated from rolling, annealing, leveling, coiling, etc. Morris et al. [3] classified the shape defects into two categories—latent and manifest. Shape defects of the latent category appear flat prior to cutting operation, whereas manifest defects, such as wavy edges and center buckles, are visible in the coiled form. Conventionally, tension levelers are used upstream to remove manifest defects. Roller leveling with lower line tension and smaller rolls has been the essential step to flatten metal strips and attenuate the effects of inhomogeneous distribution of residual stress in strips. Roller leveling is a complex forming process involving multiple, alternate bending and reverse bending cycles. In order to achieve more effective leveling operation without resorting to on site trial and error approach, a lot of efforts have been devoted to the development of efficient, accurate simulation tools for roller leveling.

Finite element analyses and analytical modeling are two main approaches adopted to investigate the roller leveling process. Hira et al. [4] developed an analytical model for

calculation of curling and residual stress of a strip in longitudinal and width directions after tension leveling. Isotropic material hardening was considered in their model. Doege et al. [5] analyzed a levelling process using the Euler–Bernoulli beam theory and a combined isotropic and kinematic hardening model. Contact points between the strip and the rolls were computed iteratively assuming that only one contact point between the roll and the strip exists. They calculated the range of roll intermeshes for zero strip curvature at the exit roll for a seven-roll leveling system. Details of the verification of their analytical modeling were not described. Behrens et al. [6] developed an analytical model to find suitable settings of a leveler for flat strips. Contact points between the metal strip and the rolls were calculated by assuming that the curve of the strip was composed of arcs and common tangents between two rolls. Lengths of several segments dissected from the strip longitudinally were equalized with different plastic deformations to eliminate wave defects of the strip. Dratz et al. [7] also adopted this common tangent contact condition to develop their roller leveling model. Residual stress and curvature results of the strip after levelling were not reported. The common tangent assumption contradicts with the fact that the curvature between two rolls exhibits a nonlinear distribution. Liu et al. [8] developed an analytical model to analyze the residual stress and curvature of a plate subjected to roller leveling. Isotropic hardening was adopted in their model and a single contact between the plate and each roll was assumed. Chen et al. [9] developed an analytical model of a roller leveler for the strip with transverse and longitudinal wave defects. They divided the strip longitudinally in order to find a suitable bending amount of the rolls to attain equal length of each longitudinal section. Higo et al. [10] presented a theoretical model for a roller leveler based on Euler–Bernoulli beam theory and a single point contact model between a strip and each roll. They examined the influence of the exit roll intermesh on the residual curvature of the strip.

Morris et al. [11] built a finite element model to analyze the deformed shape and surface residual stress of a steel strip after a three-roll leveling process. They concluded that kinematic work-hardening can represent the loading condition experienced during tension levelling more closely than that of isotropic work-hardening by comparing model predictions of the deformed shapes with experiments. Schleinzler and Fischer [12] presented a finite element model for roller leveling of rails. Combined isotropic/kinematic hardening was assumed for the material. A friction coefficient of 0.2 was used between the rail and the rolls. Park and Hwang [13] conducted finite element analyses and experiments to examine the residual curvature and stress distribution of strips after roller leveling. They verified that the strips with various initial curvatures can attain residual curvatures with small deviation given an optimum entrance roll intermesh. Huh et al. [14] built a finite element model for a roller leveler in order to study the effects of process parameters on the curvature solution of roller leveling. They identified the parameters with significant effects on the residual curvature through a design of experiment approach. Roberts et al. [15] carried out a finite element study to compare modeled curvature distributions with experiments of a two-roll stretch-bending process. Their results showed that a reduction in the wrap-around contact length was caused by decreasing intermesh. Jin et al. [16] conducted a three-dimensional finite element analysis of a roller leveler. They presented residual stress distribution in the strip. Kim et al. [17] developed a finite element model for a roller leveling process. They implemented an implicit stress integration procedure in a constitutive material model which can capture the material yield behavior and the Bauschinger effect during reverse bending. Grüber et al. [18] employed a finite element analysis of roller levelling to determine several combinations of roll intermeshes to attain a flat strip after levelling. They identified that the roll intermesh of the center load triangle and the last load triangle of a seven-roll leveler is crucial to reach desired values of flatness and residual stress distribution.

Leveler operators have relied on parameter settings for strips with various yield strengths and through-gauges provided by leveler suppliers. Due to degradation of the leveler through years of usage, empirical methods were used to fine tune the settings for production. Although manifest defects appeared to be invisible after leveling, latent

defects may still exist and cause the end products to fail to satisfy customer requirements. Analytical solutions of residual stress and curvature of the roller leveling process are necessary to provide rapid parameter settings to aid in its operation. In this investigation, an analytical model for a nine-roll roller leveler is developed. The nine-roll cold leveler was installed at the plate mill plant of the Chinese Steel Company for leveling heavy gauge steel plates. One of the motivations of this investigation is to provide operational parameters for the leveler to improve the quality of steel plates. Solutions of stress distributions after each bending/reverse bending and residual curvature of the strip are obtained based on the Euler–Bernoulli beam theory within a two-dimensional geometric framework. The material hardening is implemented through a combined isotropic/kinematic hardening parameter. Finite element analyses are carried out to verify the accuracy of the developed model. Results of the stress distributions and residual curvature of a steel strip are compared with the results based on the analyses. Finally, a roll intermesh range to produce a flatness condition of the strip is presented.

2. Analytical Model

Figure 1 is a schematic of a nine-roll leveler. The strip has the thickness t , the length L , and the width W . The rolls have a radius of R and a roll spacing of D . A strip enters the entry roll from the left, undergoes alternate bending and reverse bending, then leaves the exit roll. Flatness defects can be removed by the plastic deformation under the leveler rolls. Partial reduction in the flatness defect is ensued by insufficient plastic deformation. The intermesh settings, usually in a linear, declining trend, provide for the gradual flattening of the shape defects as the strip travels through the leveler. The roll intermeshes p_2 , p_4 , p_6 , and p_8 are indicated in Figure 1. The value of the roll intermesh is positive when the gap between the top roll and the bottom roll is larger than the strip thickness. In this investigation, the amount of the roll intermesh is defined by the inclination angle θ of the upper roll carriage and the roll intermesh at the next-to-last roll p_8 as indicated in Figure 1. The bottom rolls are fixed, and the top rolls are moved downward to specified roll intermeshes. The width of the strip is assumed to be sufficiently large. Therefore, the strain in the width direction is neglected, and the plane strain condition is considered. Since the leveling process can be viewed as a series of three-point bending/reverse bending actions with groups of three rolls, the analytical model of the roller leveling process is conducted based on the framework of Euler–Bernoulli beam theory.

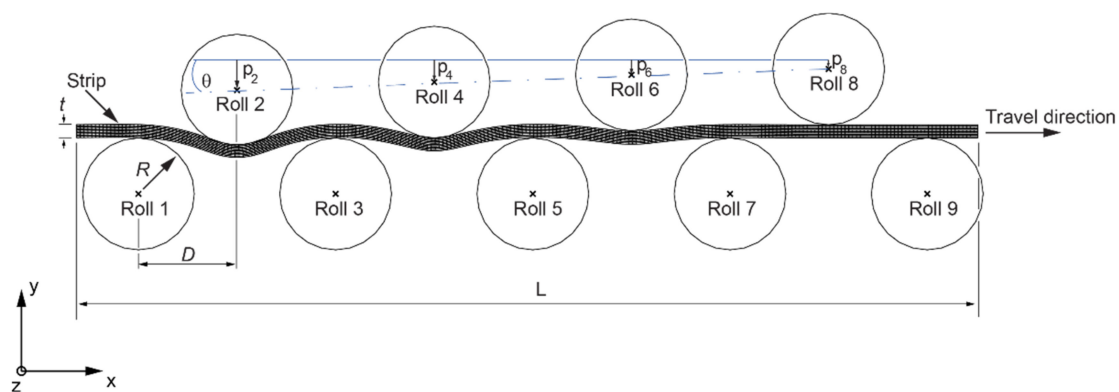


Figure 1. A schematic of a nine-roll leveler.

2.1. Material Model

In development of the analytical model, friction forces at the roll/strip interface, tension forces in the strip, and gravity are neglected. Figure 2 schematically shows a differential element of the strip. The strip has a thickness of t and a width of W . A Cartesian coordinate system is also shown in the figure. x represents the longitudinal direction, and y is along the thickness direction. The neutral axis is assumed to coincide with the mid-surface of the strip. The origin of the y coordinate is at the middle of the beam as

shown in the figure. ρ is the radius of the curvature of the differential element under the moment loading M . Longitudinal strain ε_x is expressed as

$$\varepsilon_x = -\kappa y \quad (1)$$

where ε_x and κ [1/m] are the longitudinal strain and the curvature, respectively. In the elastic regime, the longitudinal stress σ_x [N/m²] is related to the longitudinal strain ε_x by

$$\sigma_x = E\varepsilon_x \quad (2)$$

where E [N/m²] is the Young's modulus. The material hardening behavior is given by an exponential law

$$\bar{\sigma} = \sigma_s + Q_i \left(1 - e^{-b_i \bar{\varepsilon}}\right) \quad (3)$$

where $\bar{\sigma}$ [N/m²] and $\bar{\varepsilon}$ are the effective stress and the effective plastic strain, respectively. σ_s [N/m²] is the initial yield stress. Q_i [N/m²] and b_i are the isotropic hardening parameters, where Q_i specifies the maximum change in the size of the yield surface, and b_i defines the rate at which the size of the yield surface changes as plastic straining develops. For uniaxial loadings as the strip bending case, $\bar{\sigma}$ and $\bar{\varepsilon}$ can be taken as σ_x and ε_x , respectively. Relatively large plastic deformation is considered for the roller levelling. This simplification of $\bar{\varepsilon} \approx \varepsilon_x$ contributes to a very small fraction of error to the results. Values of (Q_1, b_1) and (Q_2, b_2) are obtained by fitting experimental stress–strain curve with Equation (3) for the first half cycle and the second half cycle of the loading, respectively. Therefore, Q_1 and b_1 are used to model the material hardening behavior in the first half loading cycle. Q_2 and b_2 are adopted for the subsequent loadings. The bending moment M [N·m] of the cross section of the strip is given as

$$M = -2W \int_0^{t/2} \sigma_x y dy \quad (4)$$

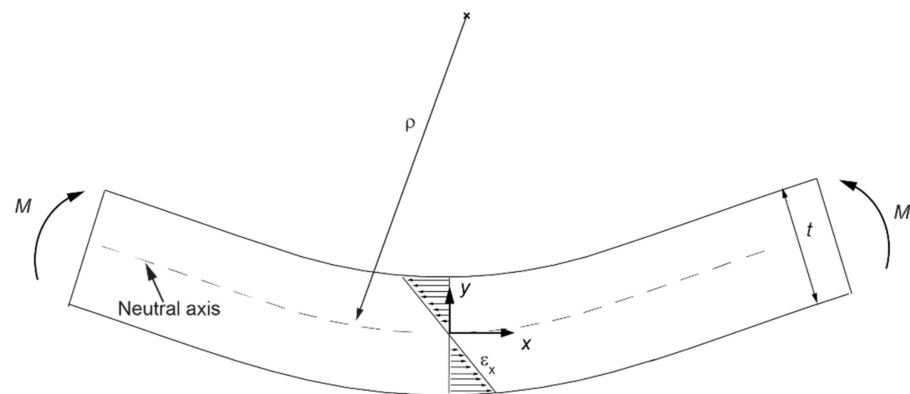


Figure 2. A schematic of a differential element of the strip.

The sign convention for the moment M and the curvature κ is related to the orientation of the coordinate axes.

During the first bend loading, the material of the strip exhibits isotropic hardening behavior. In the subsequent bend loadings, the material hardening of the strip is taken as a combined isotropic/kinematic type. Zhang et al. [19] formulated the change of the effective stress $\Delta\bar{\sigma}$ [N/m²] as a function of the change of the effective strain $\Delta\bar{\varepsilon}$ under cyclic bend loading as

$$|\Delta\bar{\sigma}| = \begin{cases} E|\Delta\bar{\varepsilon}| & , |\Delta\bar{\varepsilon}| < \frac{|\Delta\bar{\sigma}|_{\text{lim}}}{E} \\ \sigma_s + Q_i \left(1 - e^{-b_i \left(|\Delta\bar{\varepsilon}| - \frac{|\Delta\bar{\sigma}|_{\text{lim}}}{E}\right)}\right) & , |\Delta\bar{\varepsilon}| \geq \frac{|\Delta\bar{\sigma}|_{\text{lim}}}{E} \end{cases} \quad (5)$$

where $|\Delta\bar{\sigma}_{lim}|$ [N/m^2] is the elastic limit of the effective stress change at the stress reversal point and can be written as

$$|\Delta\bar{\sigma}_{lim}| = (1 + m)|\bar{\sigma}_r| + (1 - m)(2\sigma_s - |\bar{\sigma}_r|) \quad (6)$$

where $|\bar{\sigma}_r|$ [N/m^2] is the magnitude of the effective stress at the point of stress reversal. m is the combined hardening coefficient. $m = 1$ and $m = 0$ correspond to the isotropic hardening case and kinematic hardening case, respectively, and $0 < m < 1$ is for the case of combined hardening. The value of m for each bending during the roller leveling is calibrated by matching the stress–strain curves based on the model of Equations (1)–(6) to the experimental measurements in the corresponding cycles over a strain range expected in the roller leveling process. Kotov et al. [20] experimentally demonstrated the validity of a kinematic hardening model of a steel strip under roller leveling.

2.2. Contact Model

Contact points between the strip and the rolls can be computed iteratively assuming that only one contact point between the roll and the strip exists [5,10]. Behrens et al. [6] and Dratz et al. [7] adopted the common tangent contact condition to develop their roller leveling model. The single point contact and common tangent contact assumptions render a simple means to model the contact between the strip and rolls. A line contact between the strip and each roll is assumed in the initial modeling work here. In the two-dimensional model considered in this investigation, the strip contacts with each roll tangentially as shown in Figure 3. The expanded radius of the roll R_e [m] is given as

$$R_e = R + \frac{t}{2} \quad (7)$$

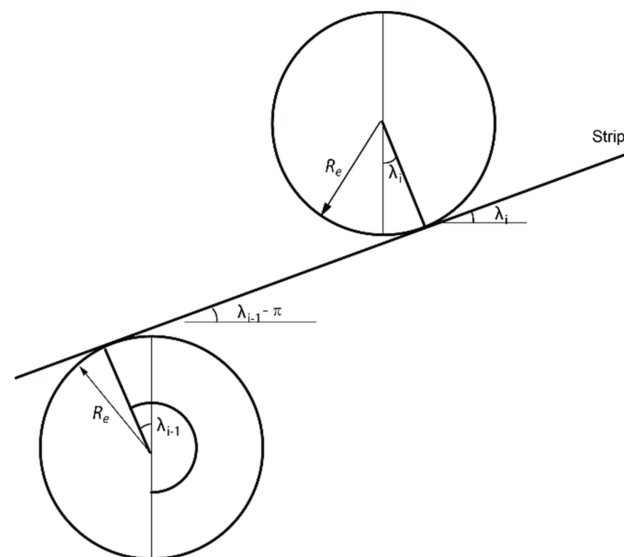


Figure 3. Tangential contact condition of the strip with the rolls.

The tangent of the contact angle λ_i [rad] is the gradient of the longitudinal axis of the strip

$$\tan\lambda_i = \left. \frac{dy}{dx} \right|_{x_i} \quad (8)$$

where $y(x)$ is the deflected curve of the longitudinal axis of the strip, (x_i, y_i) is the i th contact point, and λ_i is the i th contact angle. The contact point (x_i, y_i) [m] is

$$\begin{aligned} x_i &= x_c + R_e \sin\lambda_i \\ y_i &= y_c - R_e \cos\lambda_i \end{aligned} \quad (9)$$

where (x_c, y_c) [m] is the coordinates of the center of the roll. Müller et al. [21] also used the expanded radius of the roll to calculate the contact point between a strip and a roll in a leveler.

A recursive scheme is adopted to calculate the curvature, bending moment, deflected curve of the strip, and the contact points. Initially, the location of the contact points and the curvature κ_i of the strip curve at the i th contact point are assumed. The bending moment M_i at the i th contact point is computed using Equations (1)–(6). Based on the assumption of a linear distribution of the moment between the contact points, the curvature of the deflected strip curve is estimated. Using the curvature distribution $\kappa(x)$, the deflected strip curve y [m] is calculated by

$$y(x) = \kappa(x)dx + C_1x + C_2 \quad (10)$$

where C_1 and C_2 are the integration constants, and can be determined by the known contact points. A Newton–Raphson algorithm is used to obtain converged solutions of the deflected strip curve, moment distribution, curvature distribution, and contact points that satisfy both the Euler–Bernoulli beam theory and the geometrical constraints. Guan et al. [22] adopted a similar curvature integration approach to find the contact points for a roller leveler. They verified their model by comparing the deflection curves calculated by their model with those from experiments.

2.3. Residual Curvature

The flatness of the strip after exiting the leveler is related to the residual curvature. The bending and reverse bending cycle is repeated until the material reaches the last roll in the leveler. The strip is free to rotate at the last roll where the bending moment applied to the strip can be considered as zero. The internal stress distribution of the cross section of the strip at the last roll should result in a zero-bending moment. This condition can be enforced by imposing an artificial bending moment of the same magnitude but opposite sign to the moment at the last roll before unloading. Assuming no reverse yielding during unloading, the residual curvature κ' [1/m] of the strip at the last roll can be expressed as

$$\kappa' = \kappa - \frac{M}{EI} \quad (11)$$

where κ and M are the curvature and moment, respectively, before unloading, and I is the second moment of inertia of the cross section of the strip. Hosford and Caddell [23] and Guan et al. [24] also adopted this approach to calculate the residual curvature for beam bending problems.

3. Finite Element Analysis

In order to examine the accuracy of the developed analytical model, a two-dimensional finite element analysis of a roller leveler is carried out. A quasi-static condition is assumed in the finite element analyses. Due to the sufficiently large width, the strain in the width direction can be neglected, and the plane strain condition is considered in the finite element analysis. Both the upper and lower rolls are modeled as rigid bodies. A strip and a nine-roll leveler are shown in Figure 1. A Cartesian coordinate system is also shown in the figure. The direction of the z axis is given by the right-hand rule. In this investigation, the strip is moved forward by a displacement boundary condition and the bottom rolls are assumed to be fixed in the x and y directions and free to rotate with respect to the z axis. The displacements in the $-y$ direction of the upper rolls are specified to represent the amount of roll intermeshes, while their displacements in the x direction are constrained. As shown in Figure 1, a uniform displacement is applied in the $+x$ direction to the right edge surface of the strip, and the displacement in the y direction for the right edge surface is constrained to represent the strip travel horizontally along the $+x$ direction.

The commercial software, Abaqus (6.14, Dassault Systemes, Walthem, MA, USA), is adopted to compute the stress and deformation of the strip during the leveling process. Mises yield surface is used with the nonlinear isotropic/kinematic hardening model in Abaqus. The nonlinear kinematic hardening component is modeled through the back stress to describe the translation of the yield surface. The isotropic hardening component is modeled through the equivalent stress as a function of the equivalent plastic strain to define the size of the yield surface. The hardening law for the back stress α [N/m²] is

$$\dot{\alpha} = \frac{C}{\sigma_t} (\sigma_x - \alpha) \dot{\epsilon}^{pl} - \gamma \alpha \dot{\epsilon}^{pl} \tag{12}$$

where C [N/m²] and γ are kinematic hardening parameters that are calibrated from symmetric strain, cyclic test data. σ_t and $\dot{\epsilon}^{pl}$ are the current size of the yield surface and the plastic strain rate, respectively. Figure 4 schematically shows a stabilized cycle. The plastic strain ϵ^{pl} is determined by

$$\epsilon^{pl} = \epsilon_x - \frac{\sigma_x}{E} - \epsilon_0 \tag{13}$$

where ϵ_0 is the strain value of the intercept of the left half of the stabilized cycle with the strain axis as shown in Figure 4. The value of α [N/m²] is given as

$$\alpha = \sigma_x - \sigma_t \tag{14}$$

where $\sigma_t = (\sigma_1 + \sigma_n)/2$ is the current size of the yield surface. The stresses σ_1 and σ_n are marked in Figure 4. To solve the back stress hardening law of Equation (12) over this stabilized cycle, with the first data point of $\sigma_x = \sigma_1$ and $\epsilon^{pl} = 0$, the expression of α [N/m²] is

$$\alpha = \frac{C}{\gamma} (1 - e^{-\gamma \epsilon^{pl}}) + (\sigma_1 - \sigma_t) e^{-\gamma \epsilon^{pl}} \tag{15}$$

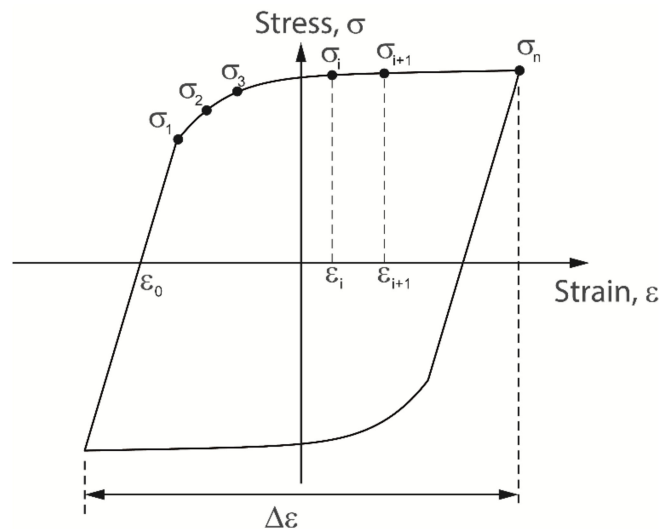


Figure 4. A schematic of a stabilized cycle.

Data pairs of (α, ϵ^{pl}) extracted from the stabilized stress–strain curve are used to calibrate values of the kinematic hardening parameters C and γ .

The isotropic hardening model of the Abaqus is defined as

$$\sigma_t = \sigma_s + Q_\infty (1 - e^{-b \bar{\epsilon}^{pl}}) \tag{16}$$

where σ_t [N/m²] and σ_s [N/m²] are the current size and the initial size of the yield surface, respectively, and $\bar{\varepsilon}^{pl}$ is the equivalent plastic strain. Q_∞ [N/m²] and b_i are the isotropic hardening parameters of the finite element model. The isotropic hardening parameters are calibrated from the data of the current size of the yield surface σ_t -equivalent plastic strain $\bar{\varepsilon}^{pl}$ relation based on a symmetric strain-controlled cyclic experiment with strain range $\Delta\varepsilon$ as shown schematically in Figure 4. For the i th cycle, the current size of the yield surface σ_t [N/m²] is calculated by

$$\sigma_t = \sigma_i^p - \alpha_i \quad (17)$$

where σ_i^p [N/m²] and α_i [N/m²] are the peak tensile stress and the back stress, respectively, in the i th cycle. α_i [N/m²] is calculated by

$$\alpha_i = \frac{\sigma_i^p + \sigma_i^n}{2} \quad (18)$$

where σ_i^n [N/m²] is the compressive stress with the same ε^{pl} value as the peak tensile stress σ_i^p in the i th cycle. Since the value of the back stress α_i in each cycle at a particular strain level is nearly the same based on the model, α_i is approximated by the values of σ_1^p and σ_1^n . The equivalent plastic strain $\bar{\varepsilon}^{pl}$ corresponding to the i th cycle is

$$\bar{\varepsilon}^{pl} = \frac{4i - 3}{2} \Delta\varepsilon^{pl} \quad (19)$$

where $\Delta\varepsilon^{pl}$ can be approximated by $\Delta\varepsilon - 2\sigma_1^p/E$.

Figure 5a is a mesh of the finite element model. Two-dimensional plane strain 4-noded CPE4R element is employed in the model. The total number of elements is 8188. Figure 5b is a close-up view of the mesh near a work roll. Ten elements are used in the thickness direction of the strip in order to obtain an accurate solution of the stress–strain distribution. The “analytical rigid surface” in Abaqus is used to model the rolls. Frictionless contact is assumed at the interface between the strip and the rolls.

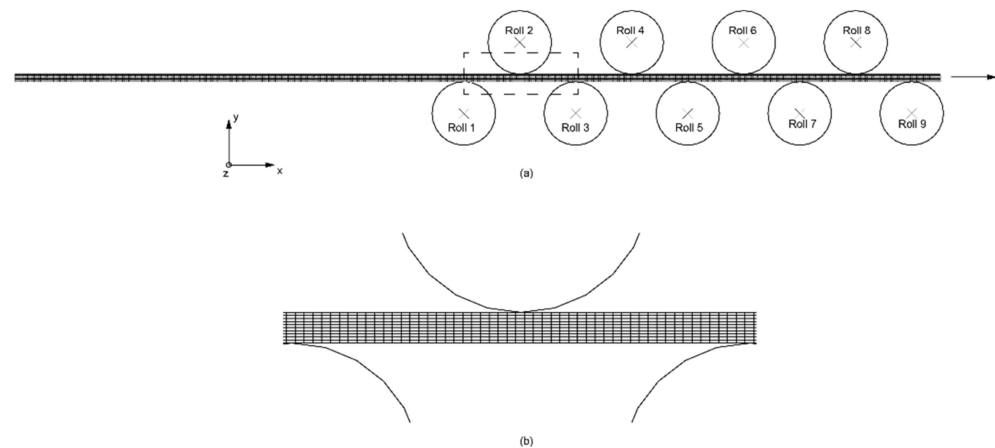


Figure 5. (a) A finite element model. (b) A close-up view of the mesh near a roll.

4. Analyses, Results, and Discussions

4.1. Analysis and Results of the Analytical Model

Figure 6 shows the stress–strain curves of a mild steel under a uniaxial, symmetric strain-controlled, cyclic test. The strain range $\Delta\varepsilon$ is 0.015. Based on the first half of the stress–strain curve of the first cycle, the calibrated values of the Young’s modulus E and the initial yield stress σ_s are 219.8 GPa and 329.7 MPa, respectively, and Q_1 and b_1 have values of 66.3 MPa and 742.7, respectively. The values of Q_2 and b_2 are calibrated as 128.3 MPa and 604.7, respectively, based on the second half of the stress–strain curve of the first cycle.

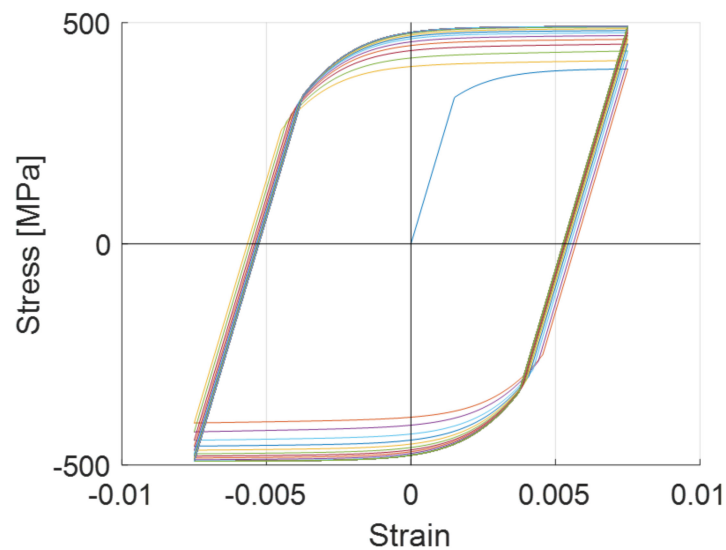


Figure 6. Stress–strain curves of a uniaxial, symmetric strain-controlled, cyclic test.

By specifying the combined hardening coefficient m , computational stress–strain curves based on the analytical model of Equations (1)–(11) with the strain range $\Delta\varepsilon$ of 0.0015 can be obtained. For a nine-roll roller leveler, the total number of bends equals seven. The values of the combined hardening coefficient m for the seven bends can be calibrated by comparing the computational stress–strain curves with the stress–strain curves of the mild steel shown in Figure 6 for the first seven bend loadings. Figure 7 shows the computational stress–strain curves and the stress–strain curves of Figure 6. The computational curves agree with those of the mild steel. The calibrated m values for the second to the seventh bending are 0.0784, 0.2, 0.3, 0.4, 0.45, and 0.5, respectively. The hardening behavior of the material for the first bending is taken as isotropic.

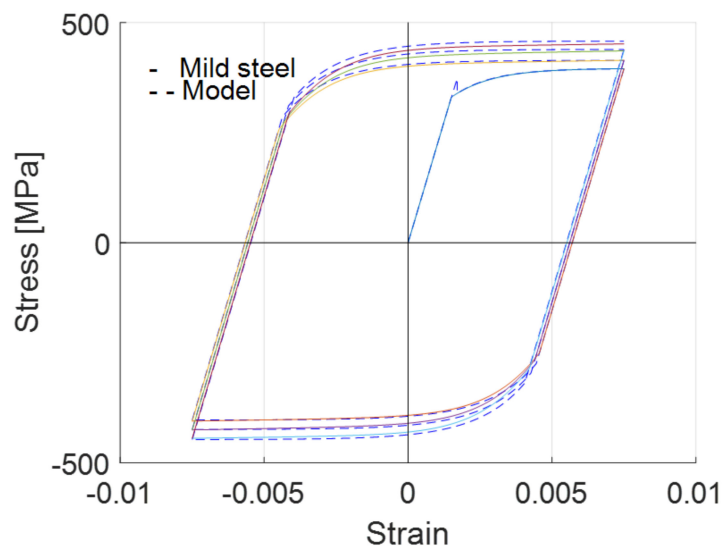


Figure 7. Stress–strain curves for calibration of the combined hardening coefficients.

Consider the case where the strip has the thickness t (=20 mm), the length L (=2480 mm), and the width W (=100 mm). The radius R of the rolls is 85 mm. The roll spacing D is 150 mm. The strip is taken as flat and free of residual stress. The upper roll carriage has an inclination angle θ of 0.1° and the roll intermesh at the next to the last roll p_8 ranges from -1.2 mm to 0.8 mm. Note that the value of the roll intermesh is positive when the gap between the top

roll and the bottom roll is larger than the strip thickness. Therefore, a negative value of the intermesh means the work roll plunges into the strip.

With $p_8 = -0.70$ mm and the upper roll carriage inclined at the angle θ of 0.1° , p_2 , p_4 , and p_6 have values of -2.32 mm, -1.78 mm, and -1.24 mm, respectively. Sixty divisions are taken along the thickness direction of the strip for calculation of the stress and strain distributions. Figure 8 shows the deformed strip between roll 1 and roll 9 based on the analytical model. Figure 9a–c shows the distribution of the bending moment per unit width, the curvature, and the deformed center line of the strip, respectively, between roll 1 and roll 9. The contact points between the strip and the rolls are marked by circles in the figure. One hundred nodes are used between the contact points in the computations. Figure 9a shows the linear distribution of the bending moment between the contact points. At the entry roll and the exit roll, the values of the bending moment are zero. Figure 9b shows the curvature distribution. Values of the curvatures are nearly two orders smaller than the roll curvature $1.176 \times 10^{-2} \text{ mm}^{-1}$. The curvature of the strip at the exit roll has a value of $3.054 \times 10^{-5} \text{ mm}^{-1}$. The positive value of the curvature indicates that the strip is bent upward. Higo et al. [10] pointed out that the abrupt increase in magnitude of the curvature near all contact points except the final one is due to the nonlinear material hardening behavior. This is evidenced by the nonlinear sections of the moment–curvature curves during the leveling process plotted in Figure 10. The moment and the curvature are normalized by the maximum bending moment M_0 and the maximum curvature C_0 for which elastic conditions hold, respectively.

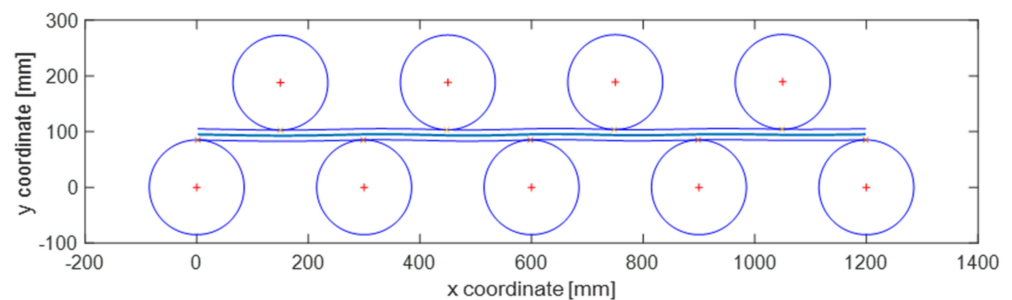


Figure 8. The deformed strip between roll 1 and roll 9.

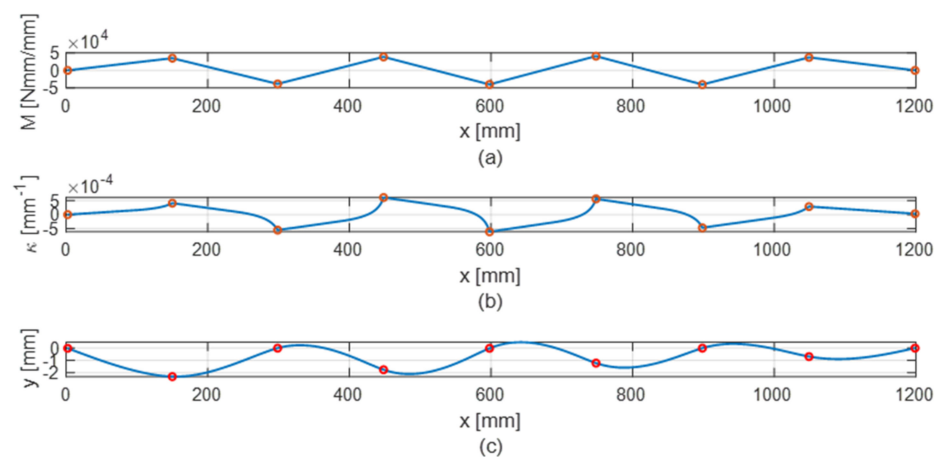


Figure 9. Distributions of (a) bending moment per unit width, (b) curvature, and (c) deformed center line of the strip between roll 1 and roll 9.

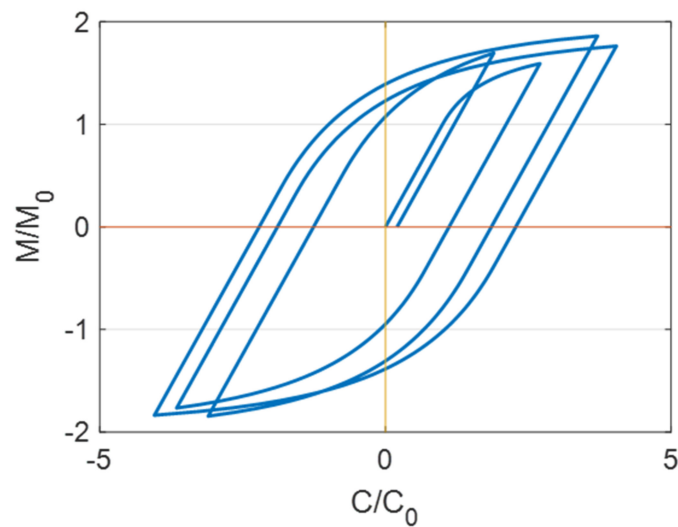


Figure 10. Normalized moment as a function of normalized curvature during leveling.

Figure 11a–c shows the stress distributions in the strip thickness direction when the strip travels through the leveler. The results computed by the analytical model are displayed by lines in the figure. Significant plastic deformations appear in the first three bends as seen in Figure 11a. The fractions of the plastic deformation are nearly 40%, 50%, and 60% for the first, the second, and the third bend, respectively. As the strip traverses through the fifth roll and the sixth roll, the region of plastic deformation stays at 60% as seen in Figure 11b. Figure 11c shows the stress distributions in the strip thickness direction at the eighth roll and the exit roll. The stress distribution at the exit roll can be taken as the residual stress distribution since the total moment applied to the strip at the exit roll is nearly zero. The stress at the i th roll is calculated based on a linear superposition assumption. The remnant stress of the cross section of the strip at the $(i - 1)$ th roll and the loading stress at the i th roll are superimposed to obtain the stress distribution at the i th roll. Guan et al. [25] also adopted this stress inheritance law in their roller leveling model. Yonetani [26] reported that the stress of a microscopic segment at the cross section in a uniaxial stress state satisfies the linear superposition assumption. The uniaxial stress loading condition is also assumed in the model considered in this investigation.

4.2. Analysis and Results of the Finite Element Model

Finite element analyses are carried out to verify the accuracy of the analytical model. The material properties for the mild steel used in the finite element analyses are listed in Table 1. The isotropic hardening parameters, Q_∞ and b , and the kinematic hardening parameters, C and γ , are calibrated from the uniaxial, symmetric strain-controlled, cyclic test with the strain range $\Delta\varepsilon$ of 0.015 as shown in Figure 6. The calibration procedure is described in Section 3.

Table 1. Material properties employed in the finite element analyses.

Property	E (Gpa)	σ_s (MPa)	Poisson's Ratio	C (Mpa)	γ	Q_∞ (Mpa)	b
Value	219.8	329.7	0.3	44,600.6	673.1	96.9	12.7

The strip is taken as flat and free of residual stress in the beginning of the leveling process. Smith [27] reported that the initially flat condition is useful in the leveling analysis since the incoming flatness defects of a strip may vary from one location to another, and a strip generally has some initially flat area. Figure 12a shows the initial configuration of the finite element model. A Cartesian coordinate system is also shown in the figure. A displacement of 1200 mm in the $+x$ direction is given to the right edge surface of the

strip. The displacement equals the distance from the center of roll 1 to the center of roll 9. Therefore, the cross-section A (marked in Figure 12a) travels from roll 1 at the beginning of the analysis to roll 9 at the end of the analysis. The y -displacement of the nodes at the right edge surface is constrained to represent the horizontal motion of the strip. Figure 12b shows the deformed shape of the mesh when the cross-section A reaches roll 9. Then, the constraints at the right edge surface of the strip are released for the strip to spring back. Figure 12c shows the deformed shape of the mesh after spring-back.

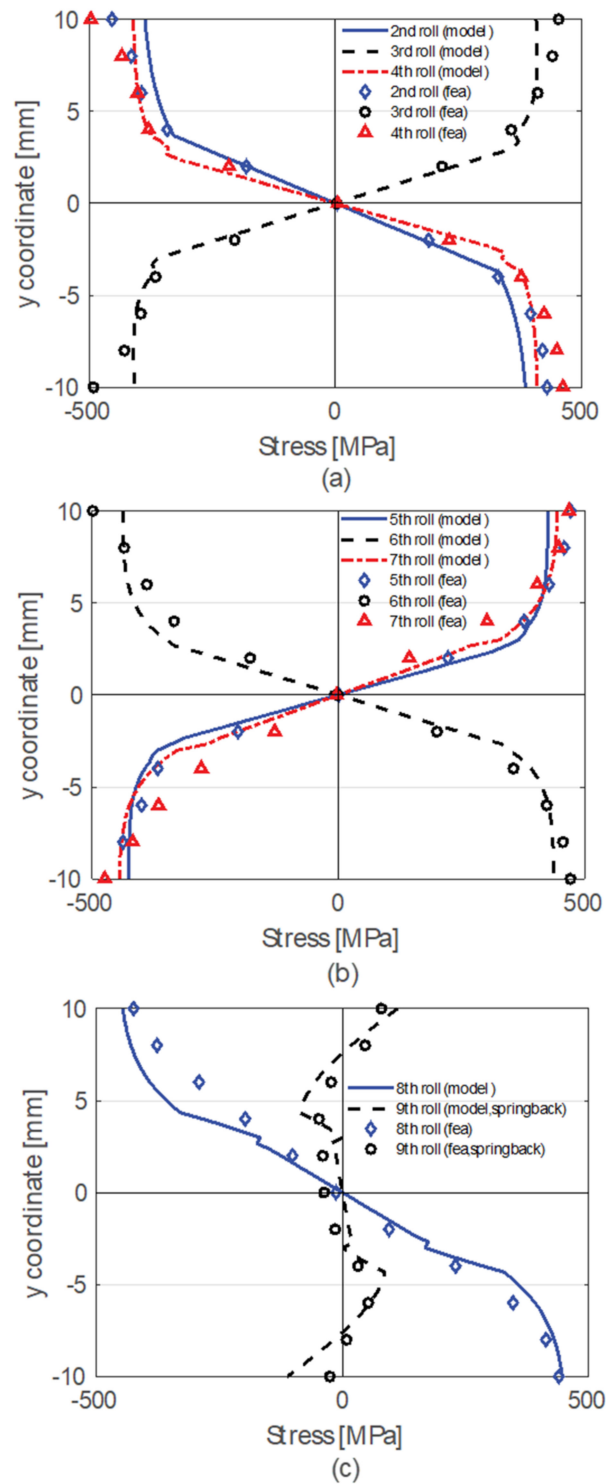


Figure 11. Stress distributions of the strip at (a) rolls 2, 3, and 4; (b) rolls 5, 6, and 7; (c) rolls 8 and 9.

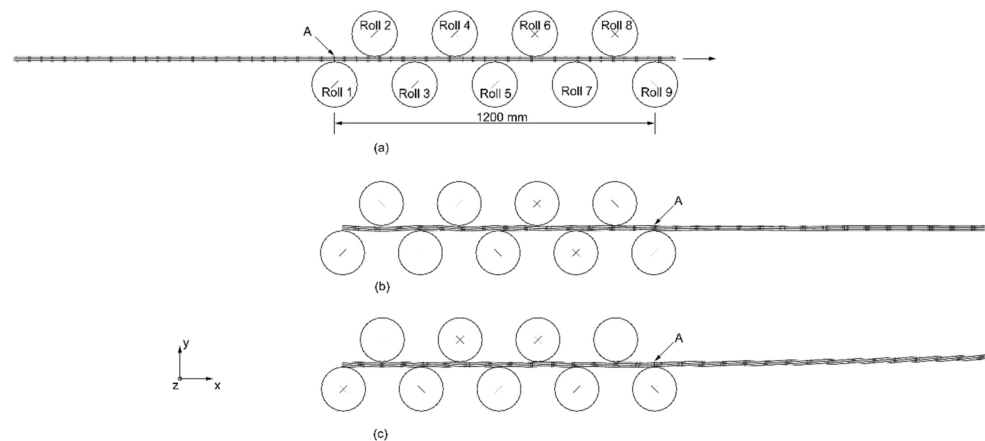


Figure 12. (a) The initial configuration, (b) a deformed configuration before spring-back, and (c) a deformed configuration after spring-back of the finite element model.

The stress distributions of the cross-section A at rolls 2–4, rolls 5–7, and rolls 8–9 based on the finite element analyses are shown in Figure 11a–c, respectively. The results based on the finite element analyses (FEA) are plotted with the markers in the figure. As shown in the figure, the analytical results agree with the results of finite element analyses. The discrepancy can be attributed to different contact conditions between the analytical model and the finite element model. Multiple contact points between the strip and each roll are observed in the finite element model. However, a single contact point between the strip and each roll is assumed in the analytical model.

4.3. Residual Curvature

Flatness is an important factor to evaluate the strip quality after roller leveling processes. The residual curvature of the strip at the exit roll can be used as a metric to evaluate the strip flatness after leveling. Figure 13 shows the residual curvatures κ' of the strip as a function of the averaged intermesh based on the analytical model and the finite element analyses. The averaged intermesh is the averaged value of the roll intermeshes, p_2 , p_4 , p_6 , and p_8 , where p_8 ranges from -1.2 mm to 0.8 mm. The residual curvature κ' is an indicator of the deviation of the strip from an initially flat surface at the entry roll. The curve with the dash-dot line and the markers represent the results based on the analytical model and the finite element analyses, respectively. The analytical predictions generally agree with the finite element analyses for the averaged intermeshes ranging from -1.71 mm to 0 . As the averaged intermesh decreases from zero, the values of κ' decreases. κ' appears to exhibit an oscillatory behavior when the averaged intermesh is less than -0.11 mm based on the analytical model. As the averaged intermesh decreases further, the amplitude of the oscillation of κ' grows. When the averaged intermesh is less than -1.41 mm (analytical predictions), κ' has positive values of increasing magnitude. Five crossover points are observed at the averaged intermesh of -0.36 mm, -0.61 mm, -0.86 mm, -1.11 mm, and -1.41 mm (analytical predictions). Smith [27] reported that the several crossover points with zero residual curvature underlie the reason why successful leveling can be achieved by the series roll leveling process in practice.

In the analytical model, a point contact is assumed between the strip and each roll, which means the strip does not wind around the work rolls. This contradicts with the fact that multi-point contact between the strip and the roll predicted in the finite element analyses. Morris et al. [3] reported that the wrap angle near the exit roll has a significant influence on the flatness of the strip. Wrap-around contact length between the strip and the roll may depend on the intermesh and roll spacing. In describing the arc of contact of the strip around a roll, an effective radius can be assumed to model the wrap-around contact characteristics. The concept of the effective radius is illustrated schematically in Figure 14. Figure 14a shows the original contact model, where the strip contacts with roll i

tangentially. R_e is the expanded radius of the roll, which is defined by Equation (7). (x_i, y_i) is the i th contact point, and λ_i is the i th contact angle. Figure 14b shows that the strip makes contact elastically with roll i when subjected to an external force F_i . The circumferences of the deformed roll and the original roll are represented by the solid line and the dashed line, respectively, in Figure 14b. (x'_i, y'_i) is the i th contact point, and λ'_i is the i th contact angle for the Hertz contact model. A local deformation is ensued to cause a reduction in the local radius of roll i . The effective radius of the roll R_s is given as

$$R_s = R_e - sF_i \quad (20)$$

where s is the contact compliance of roll i . The external force F_i is computed from the moment distribution in the analytical model. Based on the Hertz contact model, the contact point (x'_i, y'_i) is

$$\begin{aligned} x'_i &= x_c + R_s \sin \lambda'_i \\ y'_i &= y_c - R_s \cos \lambda'_i \end{aligned} \quad (21)$$

where (x_c, y_c) is the coordinates of the center of the roll. As shown in Figure 14b, the deformed center line of the strip based on the analytical model with the Hertz contact compliance may be thought to have an arc segment bounded by the two virtual contact points, U and V , wrapped around the circumference of the original roll i , shown as a dashed circle in Figure 14b. When the contact angle λ'_i is very small which is the case in the roller leveler, the line segment and the arc segment bounded by the two end points U and V are approximately equal. The contact compliance of the rolls is taken as a fitting parameter in the analytical model with the Hertz contact compliance to fit the analytical predictions with the finite element computations. Yi et al. [28] considered the wrap angle on a roll during a roller leveling process by fitting an arc curve around a roll. A parameter determined by experiments is needed for curve fitting.

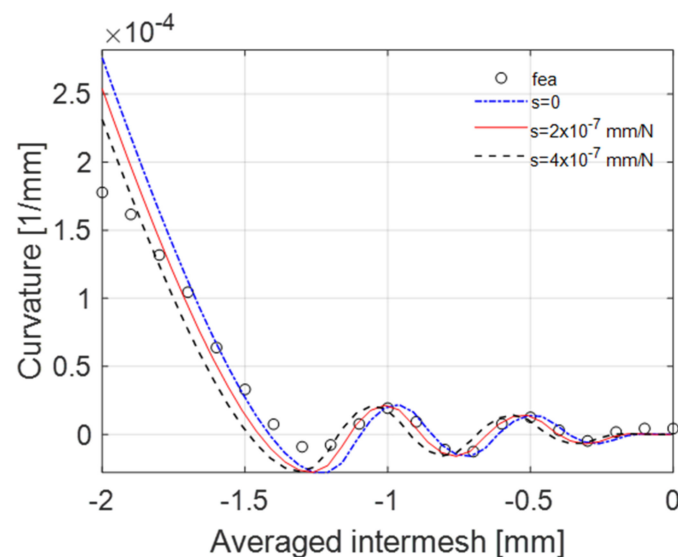


Figure 13. Residual curvature as a function of the averaged intermesh.

The residual curvatures κ' of the strip calculated by the analytical model with the Hertz contact compliance are plotted in Figure 13. The curves with the compliance $s = 0$ and $4 \times 10^{-7} \text{ mm/N}$ appear to envelop the results based on the finite element analyses. The curve with the compliance $s = 2 \times 10^{-7} \text{ mm/N}$ may be able to predict the general trend of the results based on the finite element analyses for the averaged intermesh ranging from 0 mm to -2 mm. The wrap-around contact condition between the strip and the rolls can be manifested by the analytical model with the Hertz contact compliance within an acceptable accuracy, compared with the results of the finite element analyses.

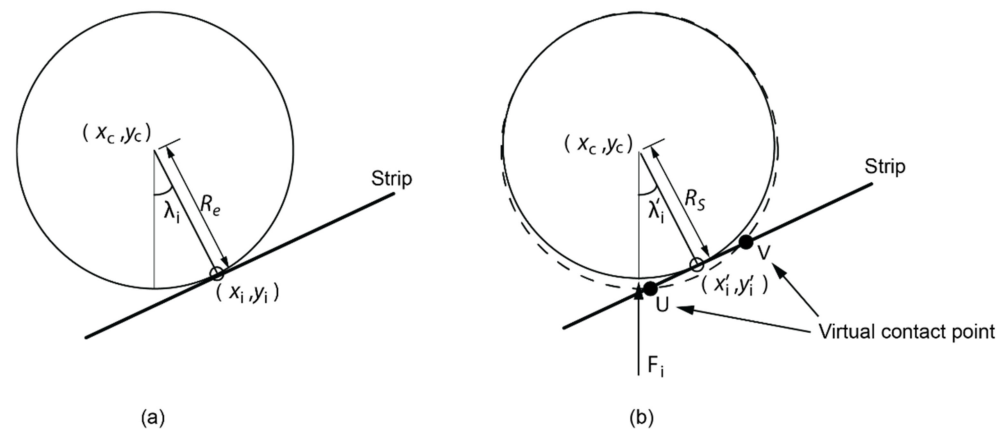


Figure 14. Illustration of (a) the original contact model; (b) the Hertz contact model.

A series of simulations was run to calculate the residual curvatures κ' of the strip with an initial curvature κ_0 based on the analytical model with the Hertz contact compliance $s = 2 \times 10^{-7}$ mm/N. The initial stress in the strip is neglected without losing generality of the residual curvature predictions. Mathieu et al. [29] considered initial flatness defects in their finite element analyses of a leveling process. They introduced the flatness defects in the strip which was free of stress. Figure 15 shows the residual curvature as a function of the averaged intermesh for the strip with the initial curvature κ_0 varying between -1×10^{-4} mm $^{-1}$ to 1×10^{-4} mm $^{-1}$. As shown in Figure 15, at low levels of roll intermesh (averaged intermeshes greater than -0.1), the residual curvatures κ' for the three cases of $\kappa_0 = -1 \times 10^{-4}$ mm $^{-1}$, 0 , and 1×10^{-4} mm $^{-1}$ deviate from each other significantly. For the averaged intermesh in this level, the curve for the case of $\kappa_0 = -1 \times 10^{-4}$ mm $^{-1}$ oscillates mostly in the positive-curvature region ($\kappa' > 0$), in contrast to the cases of $\kappa_0 = 0$ and 1×10^{-4} mm $^{-1}$, which oscillate between the positive κ' region and the negative κ' region. The initially bowed-down defect for the strip with $\kappa_0 = -1 \times 10^{-4}$ mm $^{-1}$ exits the leveler with the residual curvature in the same direction for the averaged intermesh greater than -0.71 . As the extent of the averaged intermesh increases, the residual curvatures for the three cases of $\kappa_0 = -1 \times 10^{-4}$ mm $^{-1}$, 0 , and 1×10^{-4} mm $^{-1}$ gradually converge to the same values. For the values of the averaged intermesh less than -1.1 , the curves for the three cases appear identical, where two cross over points with the interpolated averaged intermesh values of -1.46 and -1.13 were found. For the values of the averaged intermesh less than -1.46 , positive residual curvatures were produced. For the averaged intermesh values within the interval of -1.46 , -1.13 , the minimum of the residual curvature is -0.27×10^4 mm $^{-1}$. In this region of the leveler settings, the residual curvatures of the strip seem to be insensitive to its initial curvatures. This result can serve to the advantage of leveler operators to obtain nearly zero residual curvature for strips with various initial curvatures. Grüber et al. [18] also demonstrated robustness of the roll intermesh settings for a roller leveler regarding a change in the initial curvature. In this investigation, the plane strain condition is considered in the finite element analyses. The width-to-thickness ratio of the strip considered in the analyses is 5. Carvalho et al. [30] reported that, in order to develop near plain strain conditions, it is important to maintain a ratio of width-to-thickness greater than 5.

A combined isotropic/kinematic hardening is implemented to describe the material hardening of the strip in this investigation. Doege et al. [5] also adopted combined isotropic/kinematic hardening for their leveling model, where mathematical formulations of their hardening model were not presented. Detailed formulations of the hardening model are provided in this investigation. Doege et al. [5] presented analysis results of their model. Results of the stress distributions and residual curvature of a steel strip based on our analytical model are verified by the finite element analyses. Doege et al. [5] computed the contact points between the strip and the rolls by assuming only one contact point

between the strip and each roll. An effective radius modelling the wrap-around contact characteristics by the Hertz contact compliance is proposed to describe the arc of contact of the strip around a roll. A roll inter-mesh range to produce a flatness condition of the strip is presented based on the analytical model with the Hertz contact compliance.

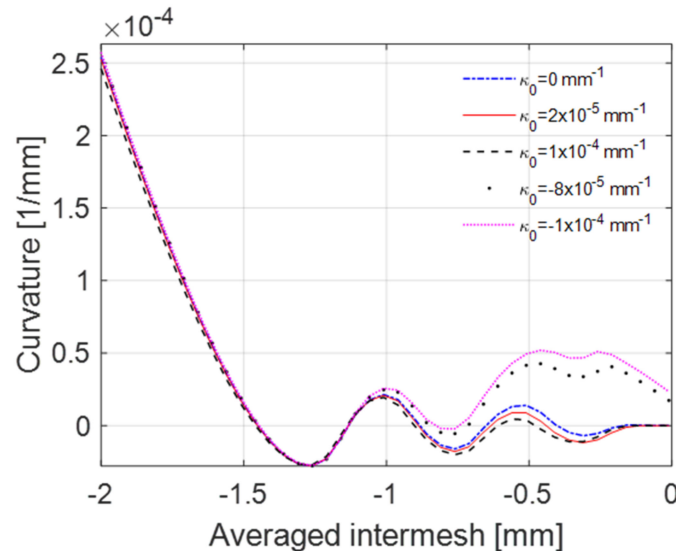


Figure 15. Residual curvature as a function of the averaged intermesh for the strip with an initial curvature.

Indeed, the initial curvature considered in the model is the longitudinal wave defect of a strip. Behrens et al. [6] sectioned a strip longitudinally and showed that the length of all sections after leveling should be the same in order to remove a transverse wave defect. Therefore, bendable rolls, as practiced in the industry, can be applied into a leveler to cause various degree of plastic deformation in each longitudinal section to achieve equal length. Chen et al. [9] developed an analytical model of a roller leveler with consideration to the bending of the rollers to eliminate transverse wave defects. This approach can be implemented in the analytical model to extend its applicability. Park and Hwang [13] slit a strip longitudinally to calculate the initial curvature of each longitudinal section. Given proper roll intermesh settings, the longitudinal sections with various initial curvatures can reach similar values of residual curvature after leveling based on finite element analyses and experiments. The results shown in Figure 15 based on the developed model also provide evidence that the residual curvatures of the strips with different initial curvatures can converge to the same value given enough amount of roll intermesh.

Given the multiple forming processes and complex machine settings involved in the roller leveling, tradeoffs between a simple, efficient model and an elaborate, detailed model should be balanced. Baumgart et al. [31] described that the effects of parts of the leveler, such as support rolls, frames, posts, and adjustment screws, should also be considered in order to obtain a more accurate leveler model. Wang and Li [32] reported that stiffness of roll cassettes and leveler housing are important factors of the leveling process. In this study, a relatively simple analytical model was developed based on the assumptions of two-dimensional geometry, pure bending of the strip, and the uniaxial loading condition. Compared to previously reported models, the Hertz contact compliance implemented in the model relaxed the single point contact condition between the strip and the roll, and a relatively accurate prediction of the residual curvature can be attained. The model could serve as a guide in the development of strategies for effective adjustment of roller levelers.

5. Conclusions

An analytical model for analyzing the residual stress distribution and residual curvatures of a strip during roller leveling is developed. The model verified by the finite element analyses is based on a simplified, two-dimensional geometric framework. The combined

isotropic and kinematic material hardening model is implemented through a combined hardening parameter. The stress distributions after each bending/reverse bending and the residual curvature at the exit roll subjected to various leveler settings can be obtained by the developed model. The model was further enhanced by considering a Hertz contact model to eliminate the discrepancies between the model predictions and the finite element analyses. Based on the analytical model with the Hertz contact compliance, a range of the leveler settings can be determined to robustly obtain a strip with a nearly zero curvature at the exit roll.

Analytical models with combined isotropic/kinematic material hardening for roller leveling have been reported previously. A formulation of the change of the effective stress as a function of the change of the effective strain under cyclic bend loading is adopted in the developed analytical model with the combined hardening. The model is efficient and accurate in predicting the stress distributions and residual curvature of a steel strip. Unlike the assumption of a single contact point between the strip and the rolls, an effective radius modelling the wrap-around contact characteristics by the Hertz contact compliance is proposed in this investigation. An arc contact of the strip around a roll is described by the Hertz contact model. A roll intermesh range to produce a flatness condition of the strip can be obtained by the analytical model with the Hertz contact compliance.

Author Contributions: Conceptualization, S.-K.K. and D.-A.W.; methodology, D.-A.W.; software, Y.-L.O.; validation, D.-A.W.; formal analysis, D.-A.W.; resources, S.-K.K.; data curation, D.-A.W.; writing—original draft preparation, D.-A.W.; writing—review and editing, D.-A.W.; funding acquisition, S.-K.K. All authors have read and agreed to the published version of the manuscript.

Funding: This research was funded by China Steel Corporation, grant number 106T7D-RE18 and the Ministry of Science and Technology, Taiwan, grant number MOST 106-2221-E-005-038.

Data Availability Statement: Data presented in this article are available at request from the corresponding author.

Acknowledgments: The authors would like to express their appreciation to the National Center for High-Performance Computing (NCHC), Taiwan for their assistance.

Conflicts of Interest: The authors declare no conflict of interest.

References

1. Amor, A.; Rachik, M.; Sfar, H. Combination of finite-element and semi-analytical models for sheet metal leveling simulation. *Key Eng. Mater.* **2011**, *473*, 182–189. [[CrossRef](#)]
2. Li, S.-Z.; Yin, Y.-D.; Xu, J.; Hou, J.-M.; Yoon, J. Numerical simulation of continuous tension leveling process of thin strip steel and its application. *J. Iron Steel Res. Int.* **2007**, *14*, 8–13. [[CrossRef](#)]
3. Morris, J.W.; Hardy, S.J.; Lees, A.W.; Thomas, J.T. Some fundamental considerations for the control of residual flatness in tension levelling. *J. Mater. Processing Technol.* **2002**, *120*, 385–396. [[CrossRef](#)]
4. Hira, T.; Abe, H.; Azuma, S. Analysis of sheet metal bending deformation behavior in processing lines and its effectiveness. *Kawasaki Steel Eng. Rep.* **1988**, *19*, 54–62.
5. Doege, E.; Menz, R.; Huinink, S. Analysis of the levelling process based upon an analytic forming model. *CIRP Ann. Manuf. Technol.* **2002**, *51*, 191–194. [[CrossRef](#)]
6. Behrens, B.-A.; El Nadi, T.; Krimm, R. Development of an analytical 3D-simulation model of the levelling process. *J. Mater. Processing Technol.* **2011**, *211*, 1060–1068. [[CrossRef](#)]
7. Dratz, B.; Nalewajk, V.; Bikard, J.; Chaste, Y. Testing and modelling the behavior of steel sheets for roll levelling applications. *Int. J. Mater. Form.* **2009**, *2*, 519. [[CrossRef](#)]
8. Liu, Z.; Wang, Y.; Yan, X. A new model for the plate leveling process based on curvature integration method. *Int. J. Mech. Sci.* **2012**, *54*, 213–224. [[CrossRef](#)]
9. Chen, W.-H.; Liu, J.; Cui, Z.-S.; Wang, Y.-J.; Wang, Y.-R. A 2.5-dimensional analytical model of cold leveling for plates with transverse wave defects. *J. Iron Steel Res. Int.* **2015**, *22*, 664–671. [[CrossRef](#)]
10. Higo, T.; Matsumoto, H.; Ogawa, S. Influence of delivery-side roll position of roller leveler to plate flatness. In Proceedings of the 2016 AISTech Conference, Pittsburgh, PA, USA, 16–19 May 2016; pp. 2129–2137.
11. Morris, J.W.; Hardy, S.J.; Lees, A.W.; Thomas, J.T. Formation of residual stresses owing to tension levelling of cold rolled strip. *Ironmak. Steelmak.* **2001**, *28*, 44–52. [[CrossRef](#)]

12. Schleinzer, G.; Fischer, F.D. Residual stress formation during the roller straightening of railway rails. *Int. J. Mech. Sci.* **2001**, *43*, 2281–2295. [[CrossRef](#)]
13. Park, K.-C.; Hwang, S.-M. Development of a finite element analysis program for roller leveling and application on removing blanking bow defects of thin steel sheet. *ISIJ Int.* **2002**, *42*, 990–999. [[CrossRef](#)]
14. Huh, H.; Heo, J.H.; Lee, H.W. Optimization of a roller levelling process for Al7001T9 pipes with finite element analysis and Taguchi method. *Int. J. Mach. Tools Manuf.* **2003**, *43*, 345–350. [[CrossRef](#)]
15. Roberts, I.; Wang, C.; Mynors, D.; Adams, P.; Lane, K.; Unwin, P. Numerical analysis of strip-roll conformity in tension levelling. In Proceedings of the 10th International Conference of Technology of Plasticity (ICTP 2011), Aachen, Germany, 25–30 September 2011; pp. 315–319.
16. Jin, H.-R.; Yi, Y.-L.; Han, X.-Y.; Liang, Y. Roller straightening process and FEM simulation for stainless steel clad plate. *Open Mech. Eng. J.* **2014**, *8*, 557–561.
17. Kim, J.; Park, K.-C.; Kim, D.-N. Investigating the fluting defect in v-bending due to the yield-point phenomenon and its reduction via roller-leveling process. *J. Mater. Processing Technol.* **2019**, *270*, 59–81. [[CrossRef](#)]
18. Grüber, M.; Kümmelb, L.; Hirt, G. Control of residual stresses by roller leveling with regard to process stability and one-sided surface removal. *J. Mater. Processing Technol.* **2020**, *280*, 116600. [[CrossRef](#)]
19. Zhang, D.; Cui, Z.; Ruan, X.; Li, Y. An analytical model for predicting springback and side wall curl of sheet after U-bending. *Comput. Mater. Sci.* **2007**, *38*, 707–715. [[CrossRef](#)]
20. Kotov, K.A.; Bolobanova, N.L.; Nushtaev, D.V. Modeling the stress state of a steel strip with a roller leveling machine under cyclic alternating deformations. *Steel Transl.* **2020**, *50*, 750–755. [[CrossRef](#)]
21. Müller, U.; Krambeer, H.; Wolff, A.; Viella, A.E.; Richardson, A.D.; Perä, J.-O.; Luoto, P.; Weberm, W. *Optimisation of Final Plate Flatness by Set-Up Coordination for Subsequent Manufacturing Process (Final Plate Flatness)*; Final Report, EUR 25852 EN; Europe Commission: Brussels, Belgium, 2013.
22. Guan, B.; Zhang, C.; Zang, Y.; Wang, Y. Model for the whole roller leveling process of plates with random curvature distribution based on the curvature integration method. *Chin. J. Mech. Eng.* **2019**, *32*, 47. [[CrossRef](#)]
23. Hosford, W.F.; Caddell, R.M. *Metal Forming—Mechanics and Metallurgy*; Prentice Hall: Hoboken, NJ, USA, 1993.
24. Guan, B.; Zang, Y.; Wu, D.; Qin, Q. Study on mechanical behavior of thin-walled member during precision straightening process. *Sens. Transducers* **2014**, *179*, 36–42.
25. Guan, B.; Zang, Y.; Wu, D.; Qin, Q. Stress-inheriting behavior of H-beam during roller straightening process. *J. Mater. Processing Technol.* **2017**, *244*, 253–272. [[CrossRef](#)]
26. Yonetani, S. *The Engender Theory and Countermeasure of Residual Stress*; China Machine Press: Beijing, China, 1983.
27. Smith, R.P. The effect of the number of leveling rolls on the straightening process. *Iron Steel Technol.* **2007**, *4*, 57–68.
28. Yi, G.; Wang, Z.; Hu, Z. A novel modeling method in metal strip leveling based on a roll-strip unit. *Math. Probl. Eng.* **2020**, *2020*, 1486864. [[CrossRef](#)]
29. Mathieu, N.; Dimitriou, R.; Parrico, A.; Potier-Ferry, M.; Zahrouni, H. Flatness defects after bridle rolls: A numerical analysis of leveling. *Int. J. Mater. Form.* **2013**, *6*, 255–266. [[CrossRef](#)]
30. Carvalho, A.P.; Reis, L.M.; Pinheiro, R.P.R.P.; Pereira, P.H.R.; Langdon, T.G.; Figueiredo, R.B. Using Plane Strain Compression Test to Evaluate the Mechanical Behavior of Magnesium Processed by HPT. *Metals* **2022**, *12*, 125. [[CrossRef](#)]
31. Baumgart, M.; Steinboeck, A.; Kiefer, T.; Kugi, A. Modelling and experimental validation of the deflection of a leveler for hot heavy plates. *Math. Comput. Model. Dyn. Syst.* **2015**, *21*, 202–227. [[CrossRef](#)]
32. Wang, X.; Li, X. Research on force simulation of main leveler housing and roll cassettes in medium and heavy plate leveling. *J. Converg. Inf. Technol.* **2012**, *7*, 153–161.